



Published in final edited form as:

J Magn Reson Imaging. 2013 November ; 38(5): . doi:10.1002/jmri.23943.

Quantification of BOLD fMRI Parameters to Infer Cerebrovascular Reactivity of the Middle Cerebral Artery

Kelley C. Mazzetto-Betti, MS¹, Renata F. Leoni, PhD^{1,3}, Octavio M. Pontes-Neto, PhD¹, Marcio J. Sturzbecher, PhD^{1,2}, Antonio C. Santos, PhD¹, Joao P. Leite, PhD¹, Afonso C. Silva, PhD³, and Draulio B. de Araujo, PhD.^{1,2,4,5}

¹Department of Neuroscience and Behavioural Sciences, FMRP, University of Sao Paulo, Ribeirao Preto, Brazil

²Department of Physics, FFCLRP, University of Sao Paulo, Ribeirao Preto, Brazil

³Cerebral Microcirculation Unit, Laboratory of Functional and Molecular Imaging, National Institute of Neurological Disorders and Stroke, National Institutes of Health, Bethesda, Maryland, USA

⁴Onofre Lopes University Hospital, Federal University of Rio Grande do Norte, Natal, Brazil

⁵Brain Institute, Federal University of Rio Grande do Norte, Natal, Brazil

Abstract

Purpose—To quantify the amplitude and temporal aspects of the BOLD response to an auditory stimulus during normocapnia and hypercapnia in healthy subjects in order to establish which BOLD parameters are best suited to infer the cerebrovascular reactivity (CVR) in the middle cerebral artery (MCA) territory.

Materials and Methods—Twenty healthy volunteers (mean age: 23.6 ± 3.7 years, 11 women) were subjected to a functional paradigm composed of five epochs of auditory stimulus (3 seconds) intercalated by six intervals of rest (21 seconds). Two levels of hypercapnia were achieved by a combination of air and CO₂ while the End-Tidal CO₂ (ETCO₂) was continually measured. An autoregressive method was applied to analyze four parameters of the BOLD signal: onset-time, time-to-peak, full-width-at-half-maximum (FWHM) and amplitude.

Results—BOLD onset time ($p < 0.001$) and FWHM ($P < 0.05$) increased linearly, while BOLD amplitude decreased ($p < 0.001$) linearly with increasing levels of hypercapnia. Test-retest for reproducibility in five subjects revealed excellent concordance for onset time and amplitude.

Conclusion—The robust linear dependence of BOLD onset time, FWHM and amplitude to hypercapnia envisages future application of this protocol in clinical studies aimed at evaluating CVR of the MCA territory.

Keywords

BOLD; fMRI; Hypercapnia; Cerebrovascular Reactivity; Auditory Stimulus; Middle Cerebral Artery

INTRODUCTION

Cerebrovascular reactivity (CVR) is an essential vasoregulatory mechanism that allows maintenance of cerebral blood flow (CBF) within a safe range to protect brain tissue against changes in blood pressure and increases of regional metabolic demand, such as during neural activation. Impaired CVR predicts higher stroke risk in patients with cervical artery stenosis (1), decline in cognitive status (2), and in elderly with high risk of falling (3). Moreover, cerebrovascular diseases significantly reduce CVR, altering neurovascular coupling (4).

Recently, Blood Oxygenation Level-Dependent (BOLD) fMRI contrast has been used successfully to investigate CVR in normal and pathological conditions (1,5). Specifically, CVR as derived from BOLD measurements is defined as the change in BOLD signal in response to manipulating the arterial partial pressure of carbon dioxide (PaCO₂), and provides a measure of the brain microvasculature capacity to react to CO₂, a potent vasodilator. BOLD-CVR investigations have been conducted using two main methods: based on dynamic changes in PaCO₂ (6–8); or based on a focal neural stimulation applied over an existing steady-state hypo- or hypercapnia condition (9). In spite of the possibility offered by both methods to evaluate brain vasomotor response, they have important differences. While the first one assesses vascular response in absence of a metabolic load, the second one assesses functional BOLD response to neural stimulation in normal conditions and under vascular stress imposed by the hypercapnic challenge.

Assessing CVR using BOLD response carries three main advantages: (i) possibility to evaluate neurovascular coupling in a specific vascular territory; (ii) usefulness in clinical practice, as it does not depend on the patient's collaboration; (iii) capability of assessing early impairments in neurovascular coupling that might precede more sensible alterations in vascular morphology or function (4).

On the other hand, robust application of BOLD-CVR in individuals with altered CVR requires a quantitative investigation of the temporal characteristics and amplitude of the BOLD signal. The goal of the present work was to develop a method capable of quantifying the amplitude and temporal characteristics of the BOLD signal in response to functional brain stimulation in brain regions supplied by the Middle Cerebral Artery (MCA). Functional MRI experiments were conducted in healthy subjects using auditory stimuli, and BOLD responses were analyzed under basal conditions and at different levels of hypercapnia.

MATERIALS AND METHODS

Twenty healthy subjects (11 female; mean age: 23.6 ± 3.7 y.o.) participated in this study. The study was approved by the local Research Ethics Committee. Informed consent was obtained from all volunteers in accordance with the institution's guidelines.

MR images were acquired on a Philips 3.0T scanner (Achieva, Philips, Best, Netherlands), using an 8-channel head coil. Anatomic images were obtained using T₁-weighted sequence (TR=6.7ms, TE=3.1ms, flip angle=8°, matrix=256×256, FOV=256mm, slices number=180; slice thickness=1mm, voxel size=1×1×1mm³, SENSE=1). Vascular anatomy of the Cerebral Arterial Circle (CAC) was inspected using magnetic resonance angiography (MRA) based on a time of flight (TOF) technique with the following acquisition parameters: TR=20ms, TE=3.5, flip angle=20°, matrix=512×512, FOV=200mm, slices number=175, voxel size=0.45×0.70×1.10mm³.

BOLD images were obtained with a gradient-echo echo-planar imaging (EPI) sequence, covering both hemispheres using the following parameters: TR=1000 ms, TE=30ms, flip angle=90°, matrix=128×128, FOV=230mm, slices number=21, slice thickness=4mm, SENSE=2.

Auditory stimuli were presented using an event-related design composed by five stimulation intervals (3 seconds each), intercalated by six intervals of rest (21 seconds each). A total of 141 volumes were acquired in each run. Three runs were conducted with the same stimulus paradigm but varying the end-tidal CO₂ (ETCO₂). In the first one, subjects breathed ambient air. In the second and third runs, ETCO₂ was increased by 5mmHg and 10mmHg, respectively. Runs were separated by at least 2 minutes to ensure steady-state conditions. The entire exam lasted approximately 20 minutes. To verify method stability, five subjects were rescanned seven days later.

An external divided nose catheter offered a mixture of air and CO₂ to the subjects while in the scanner. This catheter allowed the gas mixture to be inhaled through one nostril and the ETCO₂ to be collected through the other nostril. ETCO₂ was measured by an MRI compatible device (Veris MR, Medrad Inc., Pittsburgh, PA, USA). Pulse oxymetry and heart rate were also monitored and recorded during the exam to avoid subject hypoxia.

ETCO₂ was modulated by a dedicated micro-controlled valve system that changed the flow of inhaled CO₂. Opening and closing of the valves and the auditory stimuli presentation were controlled by a specific computational routine developed in Presentation 12.1 (Neurobehavioral Systems, Inc., Albany, CA, USA) and synchronized to the image acquisition by a parallel device that received a TTL (Transistor-Transistor Logic) signal at every excitation RF pulse.

In order to robustly modulate the primary auditory cortex, the stimulus was composed by recordings of a human male voice speaking short sentences, reproduced backwards, therefore maintaining wave amplitude and frequency components.

Data processing was performed in Brain Voyager QX 10.2™ (Brain Innovation, Maastrich, Netherlands). Pre-processing steps included motion correction, temporal correction between slices, temporal filtering using high pass filter at 0.01Hz, and spatial smoothing with Gaussian filter (FWHM=4mm) and normalization within the Talairach space.

To quantify BOLD signal characteristics, an auto-regressive method was used, which estimates four BOLD signal parameters (7): onset-time, FWHM, time-to-peak (TTP) and amplitude. The final generated colormaps represent the average value obtained from all trials in the selected volume of interest (VOI). Herein the VOI was extracted from the activated voxels (FDR<0.01) in the early auditory regions (Brodmann areas 41 and 42), resulted by the multi-subject cross correlation analysis, using a convoluted two-gama function including five lags of response delay. To better estimate FWHM, an additional method was implemented in MATLAB (2008a, MathWorks inc, Natick, MA, USA).

Statistical analysis of all BOLD parameters was conducted in GraphPad Prism 4.00 (GraphPad Software, San Diego, California, USA). Differences among all three conditions (basal, 5mmHg and 10mmHg of ETCO₂) were evaluated by a parametric one-way ANOVA with Bonferroni's multiple comparison correction. Moreover, Student-t test was performed to evaluate differences between the two hemispheres in each condition.

Anatomical variances of the CAC were also inspected and covariance analyses were conducted between the BOLD parameters and anatomical specificities. The first one

considered the variations of CAC major arteries (ACA, MCA and PCA), and the second one considered the variations of the communicant arteries.

To inspect for the stability of the protocol, Lin's concordance coefficient (10) was computed for all parameter estimates, and compared between the two consecutive sessions (re-test condition).

RESULTS

All subjects accomplished the acquisition without reporting discomfort. No images were discarded due to uncorrelated head movements.

Mean BOLD responses from the auditory cortex at different CO₂ levels, averaged across all subjects, are presented in figure 1. Figure 2 shows the color maps obtained of the mean BOLD response variables (amplitude, onset-time, FWHM and TTP) at all three ETCO₂ conditions. The responses obtained for all parameters were symmetric between hemispheres.

With increasing hypercapnic levels, there was a significant increase in onset-time and FWHM, and a significant decrease in amplitude, as shown in figure 3. The onset-time was shortest during the basal condition (right: 1.95 ± 0.16 sec, left: 1.95 ± 0.12 sec), and increased significantly during the two other levels of hypercapnia (5mmHg ETCO₂ – right: 2.54 ± 0.18 sec, left: 2.52 ± 0.18 sec; 10mmHg ETCO₂ – right: 3.01 ± 0.25 sec, left: 2.99 ± 0.21 sec, $p < 0.001$). Results from the first hypercapnic level were also statistically different from the second one ($p < 0.001$). FWHM for the two hypercapnic levels were significantly ($p < 0.01$) longer (5mmHg ETCO₂ – right: 5.89 ± 0.025 sec, left: 6.03 ± 0.25 sec, $p < 0.05$; 10mmHg ETCO₂ – right: 6.40 ± 0.32 sec, left: 6.50 ± 0.34 sec) when compared to the basal condition (right: 5.33 ± 0.18 sec, left: 5.42 ± 0.19 sec). TTP results did not present significant difference between the three ETCO₂ conditions (Fig. 3).

BOLD signal amplitude decreased significantly with increasing levels of hypercapnia. The highest BOLD amplitude was obtained under basal conditions (right: $1.77 \pm 0.09\%$, left: $1.74 \pm 0.09\%$). At ETCO₂ of 5mmHg, BOLD amplitude decreased (right: $1.38 \pm 0.06\%$, left: $1.40 \pm 0.07\%$, $p < 0.001$) and at ETCO₂ of 10mmHg it decreased further (right: $1.03 \pm 0.05\%$, left: $0.99 \pm 0.05\%$, $p < 0.001$). Statistically significant differences were also observed when comparing the two levels of hypercapnia (5mmHg and 10mmHg, $p < 0.001$) (Fig. 4).

In order to inspect the relationship between BOLD parameters and hypercapnia, a second analysis of onset-time, FWHM and amplitude was performed as a function of ETCO₂, using a linear fit. A significant positive linear correlation was observed between the increase in onset-time (right: $r^2 = 0.995$, $p = 0.04$; left: $r^2 = 0.996$, $p = 0.04$) and FWHM (right: $r^2 = 1.00$, $p = 0.003$; left: $r^2 = 0.99$, $p = 0.05$) with ETCO₂. Conversely, a negative and statistically significant linear correlation was observed between amplitude and ETCO₂ (right: $r^2 = 0.999$, $p = 0.01$; left: $r^2 = 0.999$, $p = 0.03$) (Fig. 4).

To evaluate the reproducibility of the protocol, a second session was conducted, identical to the first, in a subset of five subjects, seven days later. Lin's concordance coefficient (Rc) revealed stable results for all three parameters of interest (Fig. 4): onset-time- Rc (right) = 0.96 IC (0.5929–0.9992), Rc (left) = 0.98 IC:(0.5750–0.9994); FWHM - Rc (right) = 0.86 IC (0.5390–0.9890), Rc (left) = 0.96 IC (0.5532–0.9979); and amplitude - Rc (right) = 0.93 IC (0.6679–0.9888), Rc (left) = 0.95 IC (0.6743–0.9944).

MRA was normal in all subjects, and anatomical variations were present in posterior and anterior communicant arteries in 5 and 4 subjects, respectively. Three subjects presented

minor anatomical variations in PCA. No correlation was observed between the results present in this study and any anatomical CAC variations.

DISCUSSION

The present study investigated the correlation of specific parameters of the BOLD signal in the MCA territory with different levels of PaCO₂. Results demonstrated a linear dependence of amplitude, onset-time and FWHM with increasing hypercapnic levels. Moreover these findings were not a result of eventual anatomical variations of the CAC.

Previous works have validated BOLD response as a marker of CVR using parameters such as CBF, CBV and OEF (5,11,12), thus, to facilitate the incorporation into clinical practice, we did not use additional techniques to measure them.

Physiologically, the linearity of BOLD onset-time with ETCO₂ indicates a dependency of the initial variation of the BOLD response with the dilation state of brain arterioles in the pre-stimulus condition. In support of this hypothesis, Ainslie *et al.* reported linear influence of PaCO₂ on critical closing pressure, which, in stable situation, reflects vasomotor tone changes (13). It seems that the type of physiologic (non-neurogenic) or functional (neurogenic) task may influence the nature of vascular reactivity that governs CBF regulation (14).

The most accepted mechanism for neurogenic vasodilatation include the production local of vasoactive agents (4), however, the global vasodilatation after CO₂ inhalation results primarily from perivascular decreases in pH. Two non-excluding pathways have been described to explain non-neurogenic vasodilatation. The first one involves hyperpolarization of endothelial cells and reduction in intra-cellular Ca²⁺, leading to relaxation of pre-capillary arterioles. The other considers that acidosis causes alterations of smooth tonus by NO pathway (15). Therefore, it seems that vasodilation induced simultaneously by hypercapnia and functional stimulation is driven through potentially competitive mechanisms (14), so that the temporal characteristics of the functional BOLD signal are significantly altered by hypercapnia, as shown by our results.

The observed changes in BOLD latency with hypercapnia have relevant methodological implications, since the General Linear Model (GLM), vastly used on fMRI data, is dependent on the phase of the BOLD signal (16). Therefore, significant onset delays, possibly found in patients with a preexisting vasodilatory condition, like an exhausted cerebrovascular capacity, may lead to false negative functional responses. This problem mainly affects data analysis involving patients with cerebrovascular disorders, such as stroke survivors, that have significant alterations in BOLD response (17). Moreover, knowledge of these alterations in BOLD response allows the designing of a more efficient predictive model for GLM, minimizing such errors.

A linear correlation was also observed between FWHM and ETCO₂. Some authors have found similar results evaluating the posterior circulation (18). Behzadi and Liu (2005) modeled and concluded that an external vasodilatory stimulus causes smooth muscle relaxation, applying less radial force, while basement membrane collagen becomes tenser as the radius increases. Within the framework of the model, increased stiffness of the passive element causes a reduction in vascular responsiveness and slowing down the BOLD response (19), thus possibly leading to changes in BOLD FWHM.

The present results demonstrate a linear BOLD amplitude reduction with increasing ETCO₂ ($r^2 = 0.99$, $p=0.01$). It is worth noting that we employed a stationary state of hypercapnia before the functional task, thus causing a baseline shift, and therefore limiting the amplitude

of the BOLD response to neural stimulation (19). These results also support a recently proposed mechanism, in which the excess carbonic acid during hypercapnia reduces spiking and synaptic activity (20).

We did not observe significant differences on TTP of the BOLD response during different hypercapnic levels. Aside some previous studies have found direct relation between TTP and ETCO_2 (18), a recent study using multimodal neurovascular and neurometabolic evaluations examined the TTP of the total oxy- and deoxyhemoglobin responses did not find any statistically significant TTP differences during hypercapnia (20). In addition, a recent fMRI study in which ASL and BOLD responses to a visual task were acquired under normocapnic and hypercapnic conditions, demonstrated only a moderate transit-time reduction in gray matter during the visual stimulation under hypercapnic challenge (14).

The reproducibility of our findings was verified by a re-test session using the same protocol seven days later in 25% of the volunteers. Considering the data of same-day BOLD signal variability of the literature, our results are quite robust, conferring this protocol as a potential tool to clinical studies. The BOLD-fMRI response during hypercapnia may become an accurate and sensitive test to identify patients with disorders of brain autoregulatory mechanisms, for a better stratification of stroke risk and better selection of patients to recanalization/revascularization procedures.

The main limitation of the present study is the lack of a more direct measurement of CBF, for instance using ASL, which would certainly help to establish a direct relationship between the observed variations in BOLD parameters with CBF values. In addition, the sample studied involved primarily young adults, which provides a necessary range of normalcy of results, but may limit their extrapolation to an older population.

In conclusion, a non-invasive quantitative MR-based method was addressed as potential tool to assess CVR on the MCA territory. Results show that baseline modulation by hypercapnia produces temporal and amplitude changes in the BOLD fMRI response to a functional task. This dependence needs to be accounted for BOLD signal analysis in fMRI studies, mainly in such studies involving subjects who have any condition with potential for alteration of CVR to prevent false-negative and erroneous results. Moreover, this method may become useful to evaluate the hemodynamic capacity in patients with cerebrovascular diseases, such as inspecting for hemispheric CVR asymmetries in patients with carotid stenosis or even evaluating alterations on CVR on MCA territories after surgical or endovascular carotid intervention.

Acknowledgments

Grant Support: FAPESP 2009/08691-7

Partial Financial Support: The Intramural Research Program of the NIH, NINDS (Alan P. Koretsky, Scientific Director), CNPq and CAPES.

References

1. Mandell DM, Han JS, Poublanc J, et al. Quantitative Measurement of Cerebrovascular Reactivity by Blood Oxygen Level-Dependent MR Imaging in Patients with Intracranial Stenosis: Preoperative Cerebrovascular Reactivity Predicts the Effect of Extracranial-Intracranial Bypass Surgery. *AJNR Am J Neuroradiol.* 2011; 32(4):721–727. [PubMed: 21436343]
2. Mitschelen M, Garteiser P, Carnes BA, et al. Basal and hypercapnia-altered cerebrovascular perfusion predict mild cognitive impairment in aging rodents. *Neuroscience.* 2009; 164(3):918–928. [PubMed: 19735701]

3. Sorond FA, Galica A, Serrador JM, et al. Cerebrovascular hemodynamics, gait, and falls in an elderly population: MOBILIZE Boston Study. *Neurology*. 2010; 74(20):1627–1633. [PubMed: 20479362]
4. Girouard H, Iadecola C. Neurovascular coupling in the normal brain and in hypertension, stroke, and Alzheimer disease. *J Appl Physiol*. 2006; 100(1):328–335. [PubMed: 16357086]
5. Kassner A, Winter JD, Poulblanc J, Mikulis DJ, Crawley AP. Blood-oxygen level dependent MRI measures of cerebrovascular reactivity using a controlled respiratory challenge: Reproducibility and gender differences. *Journal of Magnetic Resonance Imaging*. 2010; 31(2):298–304. [PubMed: 20099341]
6. Andrade KC, Pontes-Neto OM, Leite JP, Santos AC, Baffa O, de Araujo DB. Quantitative aspects of brain perfusion dynamic induced by BOLD fMRI. *Arq Neuropsiquiatr*. 2006; 64(4):895–898. [PubMed: 17220991]
7. Leoni, RF.; Mazzetto-Betti, KC.; Andrade, KC.; de Araujo, DB. *Neuroimage*. Vol. 41. United States: 2008. Quantitative evaluation of hemodynamic response after hypercapnia among different brain territories by fMRI; p. 1192-1198.
8. Prisman E, Slessarev M, Han J, et al. Comparison of the effects of independently-controlled end-tidal PCO₂ and PO₂ on blood oxygen level-dependent (BOLD) MRI. *Journal of Magnetic Resonance Imaging*. 2008; 27(1):185–191. [PubMed: 18050321]
9. Liu YJ, Juan CJ, Chen CY, et al. Are the local blood oxygen level-dependent (BOLD) signals caused by neural stimulation response dependent on global BOLD signals induced by hypercapnia in the functional MR imaging experiment? Experiments of long-duration hypercapnia and multilevel carbon dioxide concentration. *AJNR Am J Neuroradiol*. 2007; 28(6):1009–1014. [PubMed: 17569947]
10. Lin LI. A concordance correlation coefficient to evaluate reproducibility. *Biometrics*. 1989; 45(1): 255–268. [PubMed: 2720055]
11. Mandell DM, Han JS, Poulblanc J, et al. Mapping cerebrovascular reactivity using blood oxygen level-dependent MRI in Patients with arterial steno-occlusive disease: comparison with arterial spin labeling MRI. *Stroke*. 2008; 39(7):2021–2028. [PubMed: 18451352]
12. Winter JD, Fierstra J, Dorner S, Fisher JA, St Lawrence KS, Kassner A. Feasibility and precision of cerebral blood flow and cerebrovascular reactivity MRI measurements using a computer-controlled gas delivery system in an anesthetised juvenile animal model. *Journal of magnetic resonance imaging*. 2010; 32(5):1068–1075. [PubMed: 21031510]
13. Ainslie PN, Celi L, McGrattan K, Peebles K, Ogoh S. Dynamic cerebral autoregulation and baroreflex sensitivity during modest and severe step changes in arterial PCO₂. *Brain Res*. 2008; 1230:115–124. [PubMed: 18680730]
14. Ho YC, Petersen ET, Zimine I, Golay X. Similarities and differences in arterial responses to hypercapnia and visual stimulation. *J Cereb Blood Flow Metab*. 2011; 31(2):560–571. [PubMed: 20700127]
15. Lindauer U, Vogt J, Schuh-Hofer S, Dreier JP, Dirnagl U. Cerebrovascular vasodilation to extraluminal acidosis occurs via combined activation of ATP-sensitive and Ca²⁺-activated potassium channels. *J Cereb Blood Flow Metab*. 2003; 23(10):1227–1238. [PubMed: 14526233]
16. Sturzbecher MJ, Tedeschi W, Cabella BCT, Baffa O, Neves UPC, De Araujo DB. Non-extensive entropy and the extraction of BOLD spatial information in event-related functional MRI. *Physics in Medicine and Biology*. 2009; 54(1):161–174. [PubMed: 19075356]
17. Mazzetto-Betti KC, Leoni RF, Pontes-Neto OM, et al. The stability of the blood oxygenation level-dependent functional MRI response to motor tasks is altered in patients with chronic ischemic stroke. *Stroke*. 2010; 41(9):1921–1926. [PubMed: 20705926]
18. Cohen ER, Ugurbil K, Kim SG. Effect of basal conditions on the magnitude and dynamics of the blood oxygenation level-dependent fMRI response. *J Cereb Blood Flow Metab*. 2002; 22(9):1042–1053. [PubMed: 12218410]
19. Behzadi Y, Liu TT. An arteriolar compliance model of the cerebral blood flow response to neural stimulus. *Neuroimage*. 2005; 25(4):1100–1111. [PubMed: 15850728]
20. Huppert TJ, Jones PB, Devor A, et al. Sensitivity of neural-hemodynamic coupling to alterations in cerebral blood flow during hypercapnia. *J Biomed Opt*. 2009; 14(4):044038. [PubMed: 19725749]

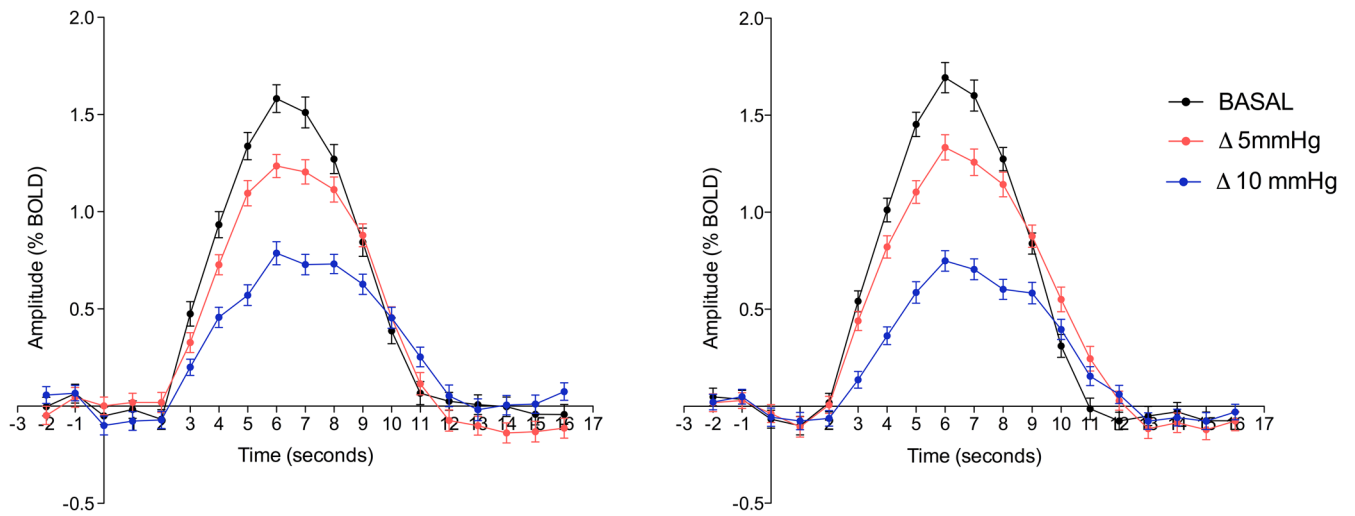


Figure 1.

Mean group BOLD time course for the right (A) and left (B) auditory cortex on the three ETCO₂ conditions: in black the basal condition, in red during an increase of 5mmHg on the ETCO₂ and in blue during an increase of 10mmHg on the ETCO₂.

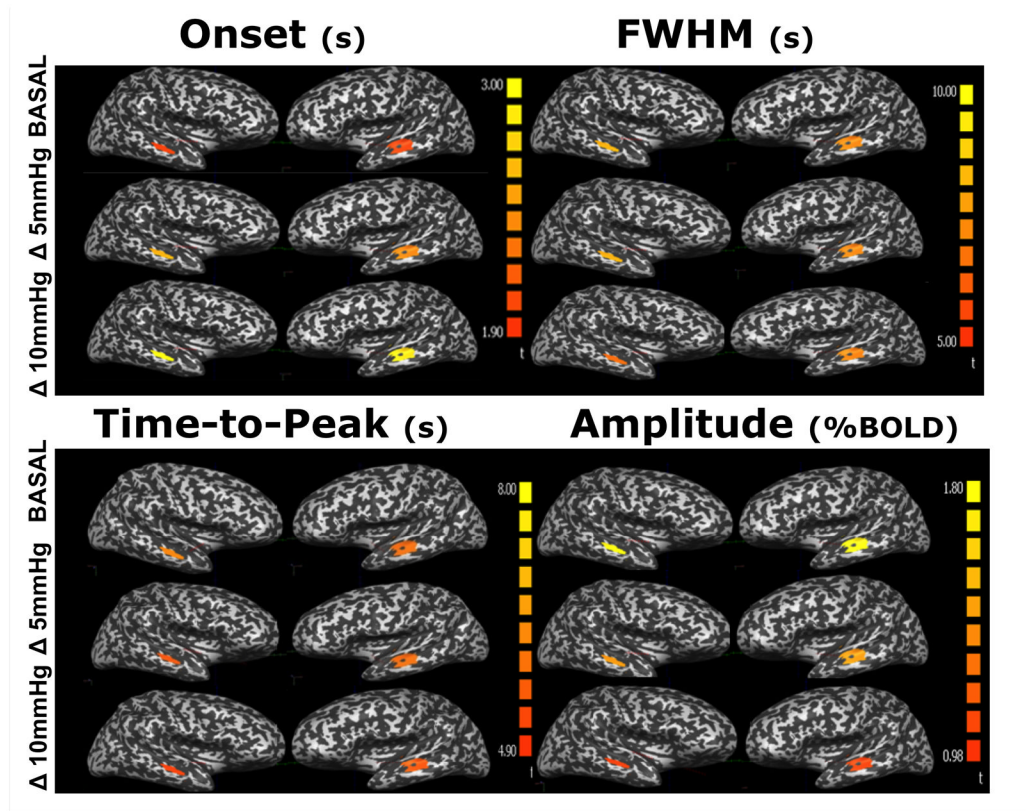


Figure 2. Colormaps of four BOLD parameters quantified during an auditory stimulus under normo- and two hypercapnic levels.

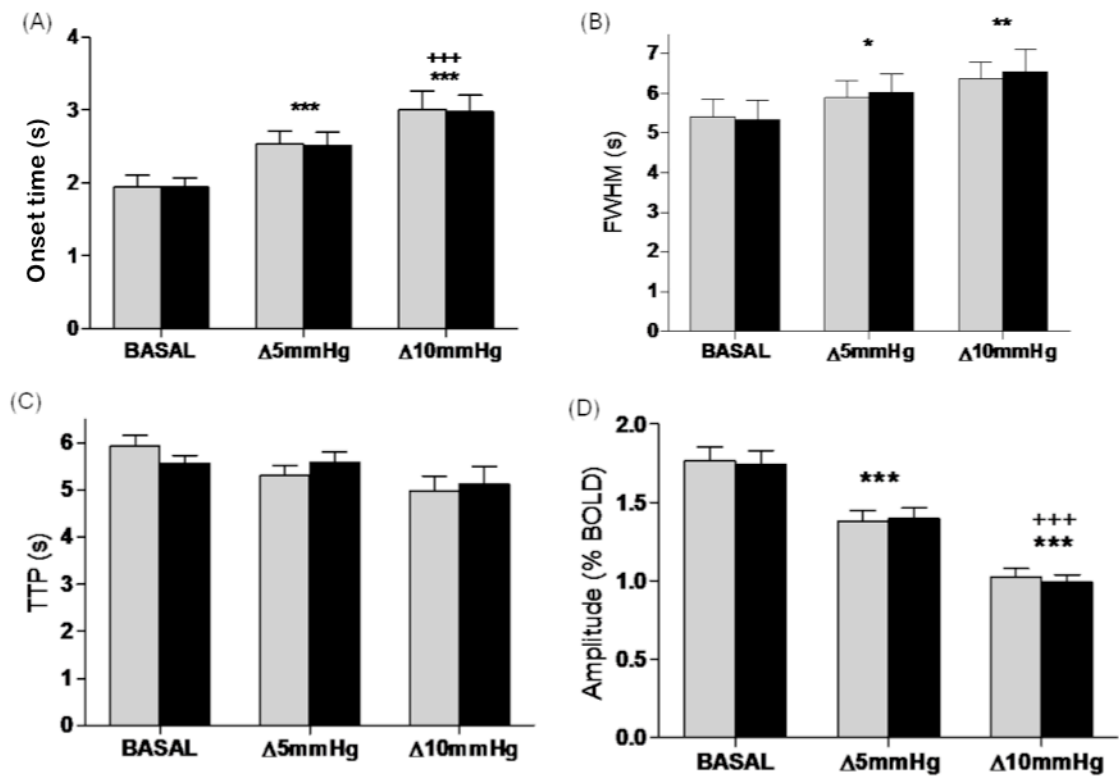


Figure 3.

The values of four BOLD signal parameters studied, in function of ETCO_2 . (A) Onset-time; (B) FWHM; (C) TTP; (D) Amplitude. Data from the right and left auditory cortices are shown in gray and black, respectively. *p < 0.05, **p < 0.01 and ***p < 0.001 compared to basal; +++p < 0.001 compared to $\text{ETCO}_2 = 5\text{mmHg}$.

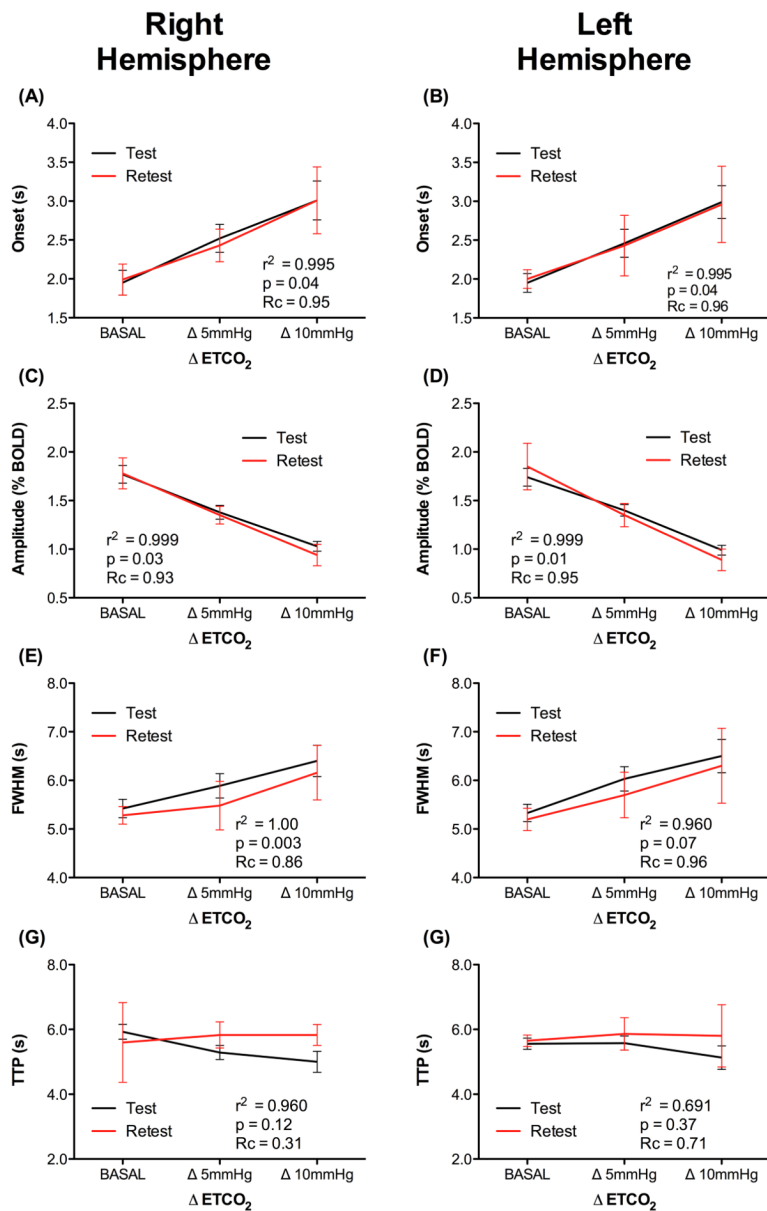


Figure 4. Linearity of the (A) onset; (B) FWHM and (C) amplitude of the BOLD HR parameters of the right and left auditory cortex.

Table 1

Mean and Stand Error (SE) of the parameters values obtained from HR during the first and second exams day.

| BASAL | | | | | | | | | | | |
|-------------------|---------|------|------|-----------------|------|---------|------|------|----------|------|---------|
| Right Hemisphere | | | | Left Hemisphere | | | | | | | |
| TEST | RE-TEST | mean | se | p value* | TEST | RE-TEST | mean | se | p value* | TEST | RE-TEST |
| Onset Time (s) | 1.95 | 0.16 | 1.99 | 0.20 | 0.60 | 1.95 | 0.12 | 2.00 | 0.12 | 1.00 | 1.00 |
| FWHM (s) | 5.42 | 0.19 | 5.28 | 0.18 | 0.42 | 5.33 | 0.18 | 5.20 | 0.23 | 0.67 | 0.67 |
| TTP (s) | 5.93 | 0.23 | 5.60 | 1.23 | 0.34 | 5.56 | 0.17 | 5.65 | 0.18 | 0.58 | 0.58 |
| Amplitude (%BOLD) | 1.77 | 0.09 | 1.78 | 0.16 | 0.43 | 1.74 | 0.09 | 1.85 | 0.24 | 0.81 | 0.81 |
| 5 mmHg | | | | | | | | | | | |
| Right Hemisphere | | | | Left Hemisphere | | | | | | | |
| TEST | RE-TEST | mean | se | p value* | TEST | RE-TEST | mean | se | p value* | TEST | RE-TEST |
| Onset Time (s) | 2.54 | 0.18 | 2.35 | 0.21 | 0.24 | 2.52 | 0.18 | 2.4 | 0.39 | 0.81 | 0.81 |
| FWHM (s) | 5.89 | 0.25 | 5.48 | 0.50 | 0.54 | 6.03 | 0.25 | 5.70 | 0.47 | 0.32 | 0.32 |
| TTP (s) | 5.29 | 0.22 | 5.83 | 0.40 | 0.28 | 5.58 | 0.22 | 5.86 | 0.50 | 0.53 | 0.53 |
| Amplitude (%BOLD) | 1.38 | 0.07 | 1.35 | 0.09 | 0.81 | 1.4 | 0.06 | 1.29 | 0.12 | 0.45 | 0.45 |
| 10 mmHg | | | | | | | | | | | |
| Right Hemisphere | | | | Left Hemisphere | | | | | | | |
| TEST | RE-TEST | mean | se | p value* | TEST | RE-TEST | mean | se | p value* | TEST | RE-TEST |
| Onset Time (s) | 3.01 | 0.25 | 3.01 | 0.43 | 0.62 | 2.99 | 0.21 | 2.96 | 0.49 | 0.87 | 0.87 |
| FWHM (s) | 6.40 | 0.32 | 6.16 | 0.56 | 0.47 | 6.50 | 0.34 | 6.30 | 0.77 | 0.45 | 0.45 |
| TTP (s) | 5.00 | 0.32 | 5.83 | 0.32 | 0.23 | 5.13 | 0.36 | 5.80 | 0.96 | 0.37 | 0.37 |
| Amplitude (%BOLD) | 1.03 | 0.05 | 0.94 | 0.11 | 0.62 | 0.99 | 0.05 | 0.89 | 0.11 | 0.44 | 0.44 |

* p value corresponds to the results of Student's T-test between TEST and RE-TEST for each condition.